ON THE MEASUREMENT OF STRUCTURE FUNCTIONS OF HIGH SCHMIDT NUMBER SCALAR IN TURBULENCE

Koji Iwano
Department of Mechanical Systems Engineering
Okayama University of Science
Ridai-cho, Kita-ku, Okayama-shi, Okayama 700-0005, Japan
k-iwano@ous.ac.jp

ABSTRACT

The concentration of a fluorescent dye with a high Schmidt number was measured on the axis of a turbulent round jet in the liquid phase. The Schmidt number and the Taylor microscale Reynolds number were 3,600 and 198, respectively. The optical fiber LIF technique, which offers a spatial resolution comparable to the Batchelor length scale, was utilized to investigate small-scale structure of the scalar field. The procedure for removing shot noise from the measured second- and fourth-order scalar structure functions is presented. The results indicate that the second- and fourth-order scalar structure functions in the direction parallel to the mean scalar gradient are proportional to r^2 and r^4 in the viscous-diffusive range, where r is the separation between two spatial points. The second−order structure function depends on r logarithmically in the viscous-convective range. The derivative flatness was estimated to about 20, which accords with the prediction based on the previous DNS results for smaller Schmidt number.

INTRODUCTION

The mixing of high Schmidt number (Sc) scalars in turbulent flows plays a crucial role in various engineering and natural phenomena. Examples include liquid phase chemical reactions, salinity mixing in the oceans, and cloud particle mixing in the atmosphere. Therefore, it is very important to understand the physics of high Schmidt number mixing.

In recent years, direct numerical simulations have been used to study high Schmidt number turbulence (Gotoh et al., 2014, Buaria et al., 2021). However, calculations, especially at high Reynolds and Schmidt numbers, are extremely challenging due to the significant computational cost.

On the other hand, the conventional experimental approaches also have a problem of the spatial resolution of concentration measurement (Miller and Dimotakis, 1996, Mohaghar et al., 2020).

For this problem, we recently developed the optical fiber LIF technique for the measurement of high Schmidt number dye with a very high spatial resolution (Iwano et al., 2021). By using the technique, we confirmed the Batchelor's -1 scaling for the power spectrum of scalar fluctuation.

For the structure of scalar field, structure functions provide richer information on the isotropy and intermittency. In experiments, the structure functions of temperature in the gas phase ($Sc \sim 1$) has been investigated (Mydlarski and Warhaft, 1998). However, to the best of the author's knowledge, there are no experimental data available for high Schmidt number cases.

The purpose of this study is to measure the concentration fluctuation of a fluorescence dye with a high Schmidt number in a round jet by using the optical fiber LIF technique and to clarify the behaviour of the scalar structure functions at small scale.

EXPERIMENTS

Figure 1 shows the schematic of the experimental apparatus and the coordinate system. The tank is 670 mm high, 680 mm wide, 2,060 mm long, and the water level is 640 mm. The axisymmetric nozzle with an exit inner diameter of 6.0 mm is fixed on the sidewall. The water solution of fluorescence dye (Rhodamine 6G) was ejected into the quiescent water in the tank. The Schmidt number of the dye was estimated to 3,600 from the water temperature during experiment. The jet Reynolds number Re_d based on the bulk exit velocity U_0 and nozzle diameter d was 20,000. The Reynolds number based on the Taylor microscale Re_λ was estimated to 198 by using the empirical formula $Re_\lambda = 1.4{Re_d}^{0.5}$ proposed by Dowling and Dimotakis (1990). The instantaneous concentration was measured by the optical fiber LIF technique, which has a spatial resolution of 2.8 μm. The measurement position was set on the jet axis at $x/d = 100$. The Kolmogorov length scale η_K and the Batchelor length scale η_B at the measurement position were estimated as 142 μm and 2.4 μm, respectively. The Batchelor length scale is comparable to the measurement spatial resolution. The output signal from the PMT was sampled with a frequency of 1 MHz after passing through the 0.5 MHz analogue low-pass filter. The experimental conditions were same as in Iwano et al. (2021) except for water temperature and sampling rate. The time series of concentration were converted to the spatial distributions by using Taylor's frozen turbulence hypothesis.

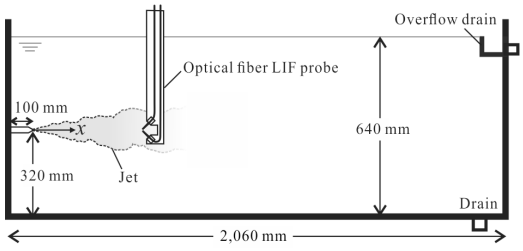

Figure 1. Schematic of experiment.

EFFECTS OF SHOT NOISE ON STRUCTURE FUNCTION MEASUREMENT

Within the framework of the LIF method, measurements capture the true concentration overlaid with shot noise, a

consequence of the particulate nature of light. This can be described as:

$$c_m = c + n \tag{1}$$

Here, c_m, c, and n represent the measured concentration, the true concentration, and the shot noise with zero mean. When considering instantaneous concentrations measured simultaneously at two distinct spatial points, x and x', the following second-order moments relation holds:

$$(c_m - c_m')^2 = (c - c')^2 + 2(c - c')(n - n') + (n - n')^2 \tag{2}$$

Here, variables with a prime $'$ correspond to values at point x', while those without are associated with point x. If the scalar concentration field is homogeneous and the noise is uncorrelated between the two points, as well as with the true concentration, then the above equation becomes:

$$S_{2m} = S_2 + 2\langle n^2 \rangle \tag{3}$$

Here, $\langle\ \rangle$ denotes time averaging and $S_{2m} = \langle (c_m - c_m')^2 \rangle$, $S_2 = \langle (c - c')^2 \rangle$. Given that true structure function S_2 is minimal for small separations, the value of $2\langle n^2 \rangle$ can be inferred from the measured structure function S_{2m}. This allows for the determination of the value of S_2. In a similar manner, for the fourth-order moments,

$$S_{4m} = S_4 + 12S_2\langle n^2 \rangle + 6\langle n^2 \rangle^2 + 2\langle n^4 \rangle \tag{4}$$

Here, $S_{4m} = \langle (c_m - c_m')^4 \rangle$ and $S_4 = \langle (c - c')^4 \rangle$. From this, the value of $2\langle n^4 \rangle$ can be deduced using S_{4m}, S_2, and $\langle n^2 \rangle$ at small separations, leading to the determination of the value of S_4.

RESULTS AND DISCUSSION

The mean scalar concentration along the jet axis decreases in the downstream direction. Since the measurement was conducted on the jet axis and the Taylor hypothesis was used in this study, it can be considered that the measured structure functions are in the direction parallel to the mean scalar concentration gradient direction.

Figure 2(a), 2(b) show S_{2m} and S_2 normalized by the variance of scalar fluctuation ${c_{rms}}^2$ in log-log plot and log-linear plot, respectively. The horizontal axis is the separation of two points r normalized by the Batchelor scale η_B. From the figure 2(a), it is clearly seen that S_{2m} takes a constant value for small r. Therefore, it is feasible to estimate the variance of the shot noise (=$2\langle n^2 \rangle$). The value of $2\langle n^2 \rangle$ was calculated by averaging S_{2m} for $r/\eta_B < 0.34$. The gray shaded area represents the $\pm 5\%$ uncertainty in estimating $2\langle n^2 \rangle$. S_2 appears to increase proportionally to r^2 around the Batchelor scale η_B, which is consistent with theoretical predictions for the viscous-diffusive range (Borgas et al., 2014, Gauding et al., 2017). Although the proportionality to r^2 is seen in $r/\eta_B < 1$, it may be affected by the measurement spatial resolution. From the figure 2(b), we can observe the structure function increase proportional to $\ln(r)$ in the viscous-convective range ($10 < r/\eta_B < 100$). This is consistent with the previous DNS results for smaller Re_λ and Sc (Borgas et al., 2004).

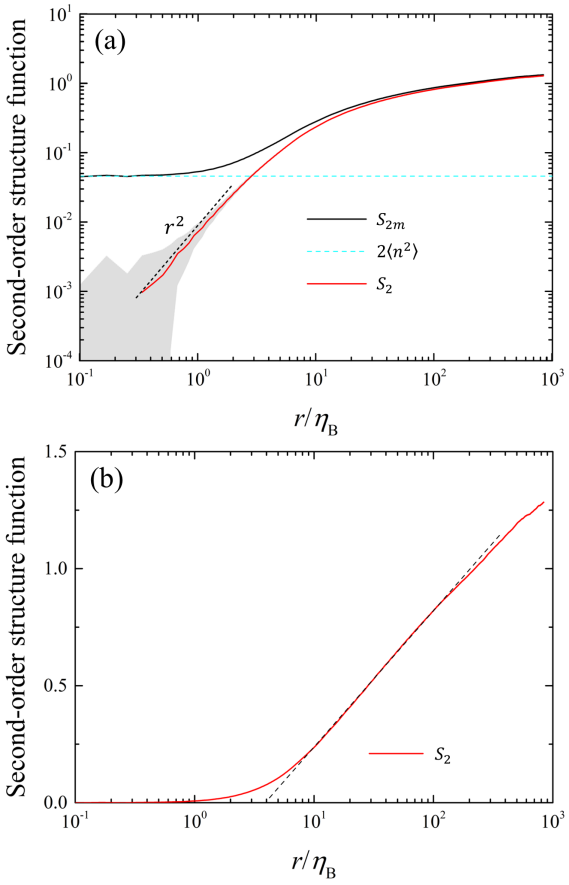

Figure 2. Second-order structure function normalized by the variance of scalar fluctuation ${c_{rms}}^2$ in (a) log-log plot and (b) log-linear plot.

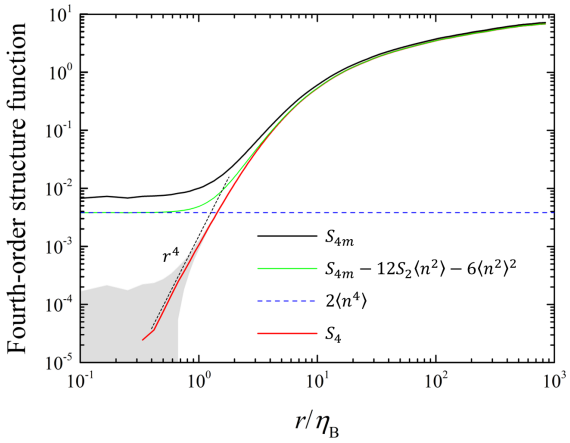

Figure 3. Fourth-order structure function normalized by ${c_{rms}}^4$.

Figure 3 shows S_{4m}, $S_{4m} - 12S_2\langle n^2 \rangle - 6\langle n^2 \rangle^2$, and S_4. All are normalized by ${c_{rms}}^4$. From the figure, we can see that $S_{4m} - 12S_2\langle n^2 \rangle - 6\langle n^2 \rangle^2$ takes constant value for small r. Therefore, we can know the value of $2\langle n^4 \rangle$, leading to determination of S_4. The value of $2\langle n^4 \rangle$ was calculated by averaging $S_{4m} - 12S_2\langle n^2 \rangle - 6\langle n^2 \rangle^2$ for $r/\eta_B < 0.34$. The gray shaded area represents the $\pm 5\%$ uncertainty in estimating $2\langle n^4 \rangle$. The result shows that S_4 increases proportionally to r^4 around the Batchelor scale η_B, which is consistent with

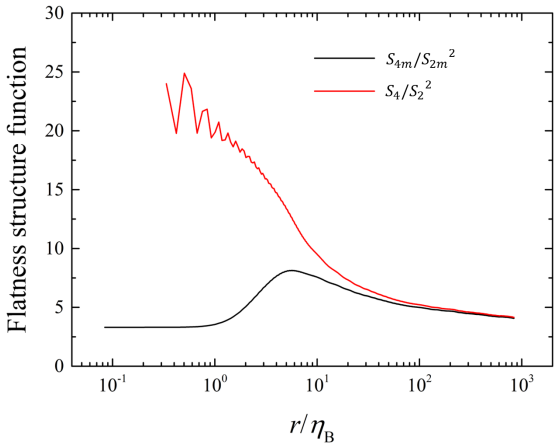

Figure 4. Flatness structure function.

theoretical predictions for the viscous-diffusive range (Gauding et al., 2017).

Figure 4 shows the flatness structure function $S_4/S_2{}^2$. As the separation tends to zero, this approaches the derivative flatness $F_{\nabla c}$. From the figure, it's discernible that before noise removal, as r decreases, it peaks around $\eta_B = 7$ and then declines. However, after noise subtraction, it continuously increases, and asymptotically approaching about 20 around $\eta_B = 1$. Although the spatial resolution might not be sufficient to determine each value of S_4 and S_2 below the Batchelor scale, $S_4/S_2{}^2$ would not be sensitive the spatial resolution since that effect is somewhat cancelled out. This has been confirmed in the case of velocity derivative flatness (Tang et al. 2018).

Based on DNS results up to $Sc = 64$, Donzis and Yeung (2010) predicted that the $F_{\nabla c}$ depends on the Reynolds number as $Re_\lambda{}^{0.244}$ and $F_{\nabla c}/Re_\lambda{}^{0.244} = 5.7$ for $Re_\lambda{}^2 Sc > 5000$. On the other hand, the present experiment shows $F_{\nabla c}/Re_\lambda{}^{0.244} = 5.5$, a value almost identical to their results, even though the $Re_\lambda{}^2 Sc$ value achieved in our experiment is two orders of magnitude larger than their numerical simulations.

CONCLUDING REMARKS

In this study, we presented experimental results on the structure function of high Schmidt number scalar in turbulent flow for the first time. The optical fiber LIF technique was utilized to measure the high Schmidt number scalar, and the behaviour of second- and fourth-order structure functions was elucidated. All the results presented here align consistently with previous studies. This finding deepens our understanding of the intrinsic mechanisms governing high Schmidt number scalar mixing.

ACKNOWLEDGEMENTS

This study was partly supported by JSPS Grant-in-Aid for Scientific Research (21K03851, 22K03937).

REFERENCES

Borgas, M.S., Sawford, B.L., Xu, S., Donzis, D.A., Yeung, P.K., 2004, “High Schmidt number scalars in turbulence: Structure functions and Lagrangian theory”, *Physics of Fluids* Vol. 16, pp. 3888–3899.

Buaria, D., Clay, M., Sreenivasan, K. R., and Yeung, P. K., 2021, " Turbulence is an Ineffective Mixer when Schmidt Numbers Are Large", *Physical Review Letters*, Vol. 126, 074501.

Donzis, D.A., Yeung, P.K., 2010, “Resolution effects and scaling in numerical simulations of passive scalar mixing in turbulence", *Physica D: Nonlinear Phenomena*, Vol. 239, pp. 1278–1287.

Dowling, D.R. and Dimotakis, P.E., 1990, “Similarity of the concentration field of gas-phase turbulent jets”, *Journal of Fluid Mechanics*, Vol. 218, pp. 109-141.

Gauding, M., Danaila, L., and Varea, E., 2017, “High-order structure functions for passive scalar fed by a mean gradient”, *International Journal of Heat and Fluid Flow*, Vol. 67, pp. 86-93.

Gotoh, T., Watanabe, T., and Miura, H., 2014, "Spectrum of Passive Scalar at Very High Schmidt Number in Turbulence", *Plasma and Fusion Research*, Iowa State Univ., Vol. 9, 3401019.

Iwano, K., Hosoi, J., Sakai, Y., and Ito, Y., 2021, " Power spectrum of high Schmidt number scalar in a turbulent jet at a moderate Reynolds number", *Experiments in Fluids*, Vol. 62, 129.

Miller, P.L., Dimotakis, P.E., 1996. “Measurements of scalar power spectra in high Schmidt number turbulent jets”, *Journal of Fluid Mechanics*, Vol. 308, pp. 129–146.

Mydlarski, L., Warhaft, Z., 1998, “Passive scalar statistics in high-Péclet-number grid turbulence”, *Journal of Fluid Mechanics,* Vol. 358, pp. 135–175.

Mohaghar, M., Dasi, L.P., Webster, D.R., 2020, “Scalar power spectra and turbulent scalar length scales of high-Schmidt-number passive scalar fields in turbulent boundary layers”, *Physical Review Fluids*, Vol. 5, 084606.

Tang, S.L., Antonia, R.A., Djenidi, L., Danaila, L., Zhou, Y., 2018, “Reappraisal of the velocity derivative flatness factor in various turbulent flows”, *Journal of Fluid Mechanics*, Vol. 847, pp. 244–265.